

# Technical Advance

## Combining GAL4 GFP enhancer trap with split luciferase to measure spatiotemporal promoter activity in *Arabidopsis*

Ángela Román<sup>1,2</sup>, John F Golz<sup>1</sup>, Alex AR Webb<sup>3</sup>, Ian A Graham<sup>2</sup>, Michael J Haydon<sup>1,2</sup>

1. School of BioSciences, University of Melbourne, Australia
2. Department of Biology, University of York, United Kingdom
3. Department of Plant Sciences, University of Cambridge, United Kingdom

Corresponding author: Michael J. Haydon (m.haydon@unimelb.edu.au)

**Running title** ETSLA: Enhancer trap-compatible split luciferase assay

### Summary

In multicellular organisms different types of tissues have distinct gene expression profiles associated with specific function or structure of the cell. Quantification of gene expression in whole organs or whole organisms can give misleading information about levels or dynamics of expression in specific cell types. Tissue- or cell-specific analysis of gene expression has potential to enhance our understanding of gene regulation and interactions of cell signalling networks. The *Arabidopsis* circadian oscillator is a gene network which orchestrates rhythmic expression across the day/night cycle. There is heterogeneity between cell and tissue types of the composition and behaviour of the oscillator. In order to better understand the spatial and temporal patterns of gene expression, flexible tools are required. By combining a Gateway®-compatible split luciferase construct with a *GAL4 GFP* enhancer trap system, we describe a tissue-specific split luciferase assay for non-invasive detection of spatiotemporal gene expression in *Arabidopsis*. We demonstrate the utility of this enhancer trap-compatible split luciferase assay (ETSLA) system to investigate tissue-specific dynamics of circadian gene expression. We confirm spatial heterogeneity of circadian gene expression in *Arabidopsis* leaves and describe the resources available to investigate any gene of interest.

### Significance statement

Cell and tissue type resolution of gene expression is important to understand functional properties of signalling networks. We have adapted a split luciferase system for use with existing collections of enhancer trap lines to provide a versatile tool to detect dynamic tissue-specific gene expression in whole *Arabidopsis* seedlings and demonstrate its utility to detect spatial heterogeneity of circadian rhythms in leaves.

## Introduction

In multicellular organisms different cell and tissue types have distinct gene expression profiles. Quantification of gene expression in whole organs or whole organisms can give misleading information about levels or dynamics of expression in specific cell types. Tissue- or cell-specific analyses of gene expression can enhance our understanding of transcriptional responses to environmental cues. The circadian clock orchestrates rhythmic gene expression according to daily environmental cues. The *Arabidopsis* core circadian oscillator is comprised of a gene network of regulatory feedback loops involving around 20 genes (Haydon *et al.*, 2019). Although most core oscillator genes are expressed in all cells, there is spatial heterogeneity of circadian gene expression in *Arabidopsis* (Para *et al.*, 2007; Xu *et al.*, 2007; James *et al.*, 2008; Wenden *et al.*, 2012; Martí *et al.*, 2013; Endo *et al.*, 2014; Takahashi *et al.*, 2015; Bordage *et al.*, 2016; Kim *et al.*, 2016; Gould *et al.*, 2018; Greenwood *et al.*, 2019).

Several techniques have been used to isolate specific cell populations from plant tissues for gene expression analyses but a common disadvantage of these is the destructive nature of sampling. Sampling protocols can alter gene expression, diminish intercellular signalling and limit resolution for temporal information. Laser-Capture Microdissection (LCM) was developed to isolate cell populations from sections of animal tissues for gene expression analyses (Emmert-Buck *et al.*, 1996; Bonner *et al.*, 1997) and has been similarly applied to plant tissues (Asano *et al.*, 2002; Kerk *et al.*, 2003; Nakazono *et al.*, 2003). RNA can be extracted from LCM samples and used for quantitative transcript analyses. Using LCM in *Arabidopsis*, circadian rhythms have been measured in shoot apices by measuring transcripts and fluorescent proteins in dissected tissues (Takahashi *et al.*, 2015). However, this technique is limited by accessibility of the tissue of interest and identifiable cell types. Similarly, a protocol was developed to isolate mesophyll, vasculature and epidermal tissues from *Arabidopsis* leaves with high purity to measure transcripts over a circadian time-course, which indicated distinct characteristics of circadian gene expression in leaf vasculature (Endo *et al.*, 2014).

Transcriptome analyses of Fluorescence Activated Cell Sorting (FACS) of protoplasted transgenic plants expressing cell type-specific GFP markers has allowed high-resolution spatial maps of transcription in *Arabidopsis* roots (Birnbaum *et al.*, 2003; Brady *et al.*, 2007; Dinneny *et al.*, 2008), and more recently adapted for leaves (Grønlund *et al.*, 2012; Coker *et al.*, 2015). However, the process of protoplasting can alter gene expression. By contrast, the INTACT method (isolation of nuclei tagged in specific cell types) uses an affinity-approach to isolate nuclei from transgenic plants expressing a cell type-specific biotinylated nuclear protein marker (Deal and Henikoff, 2011). This method has been used to determine cell type-specific nuclear transcriptomes in numerous plant species to provide spatial information about gene expression in diverse cell types (Ron *et al.*,

2014; Moreno-Romero *et al.*, 2017; Del Toro-De Leon and Kohler, 2018; Reynoso *et al.*, 2018). However, INTACT has so far not been applied to measure temporal characteristics of gene expression.

Emerging single-cell RNA sequencing (scRNA-seq) technologies have the potential to generate high-resolution maps of gene expression networks, particularly in emerging model species where specific fluorescent markers are not available (Efroni and Birnbaum, 2016). Recent studies have performed scRNA-seq on protoplasts from *Arabidopsis* root cells using droplet-based microfluidics to provide the first gene expression maps of roots of wild-type and seedlings at single-cell resolution (Ryu *et al.*, 2019; Denyer *et al.*, 2019; Jean-Baptiste *et al.*, 2019). These studies have provided high-resolution spatiotemporal maps and identified developmental waves of gene expression associated with root cell differentiation. Applications of scRNA-seq in plant systems are likely to accelerate as the technology and data analyses become more accessible.

Transgenic luciferase reporters are well-suited for measuring gene expression *in planta* with high temporal resolution. However, luminescence imaging systems typically have poor spatial resolution. A modified split luciferase system has been shown to be effective for measuring circadian rhythms specifically in phloem companion cells (Endo *et al.*, 2014). The N- and C-terminal halves of luciferase were expressed from a phloem-specific and circadian gene promoter, respectively, and the reconstituted luciferase produces luminescence only in the phloem companion cells in which both transgenes are expressed. This system allows measurement of gene expression in specific cell and tissue types but depends on availability of characterised tissue-specific promoters.

Enhancer trap screens have been effective in identifying tissue-specific enhancer elements in *Arabidopsis*. Rather than reporting activity of a full promoter, which can be regulated by multiple endogenous and environmental signals, enhancer trap lines drive reporter activity from a specific enhancer. In this way, these lines can be advantageous over tissue-specific promoters. The *GAL4 GFP* enhancer trap lines carry a transgene encoding a GAL4-VP16 transcriptional activator from yeast with a minimal promoter and a modified GFP targeted to the ER (mGFP5ER) under the control of GAL4-binding upstream activation sequences (*UAS*). Transformants have been screened for diverse spatial patterns of GFP fluorescence, driven by enhancer elements in the vicinity of the insertion regulating *GAL4-VP16* (Haseloff, 1999; Laplaze *et al.*, 2005). Unique patterns of expression have been identified for enhancer trap lines for which there is no known gene promoter (Gardner *et al.*, 2009). Characterised enhancer trap lines can be used to drive tissue-specific expression of any gene of interest from a *UAS* by introducing a second transgene by crossing or transformation. In this way, *GAL4 GFP* enhancer trap lines have been exploited to modify gene expression in specific cell types (Laplaze *et al.*, 2005; Laplaze *et al.*, 2007; Gan *et al.*,

2012) or drive cell type-specific reporters (Dodd *et al.*, 2006; Jia *et al.*, 2007; Martí *et al.*, 2013) by transactivation. There are approximately 250 *GAL4 GFP* enhancer trap lines across four sets available from stock centres and characterisation of these lines continues to increase, broadening their utility (Ckurshumova *et al.*, 2009; Radoeva *et al.*, 2016) .

We have exploited the tissue-specific variation of the circadian oscillator to develop and test the combination of a Gateway®-compatible split luciferase construct with an established GAL4 enhancer trap system (Laplaze *et al.*, 2005) for non-invasive detection of spatiotemporal gene expression in Arabidopsis. We demonstrate the utility of this enhancer trap split luciferase assay (ETSLA) system to investigate tissue-specific promoter activity and apply this to measure circadian gene expression. We confirm spatial heterogeneity of circadian promoter activity in Arabidopsis leaves and describe the resources available to investigate any gene of interest.

## Results

### *Development of an enhancer trap tissue-specific split luciferase assay (ETSLA) system*

To measure gene expression in specific tissues in *Arabidopsis* we set out to adapt a split luciferase system to be applicable with existing *GAL4 GFP* enhancer trap lines (Figure 1). Enhancer trap lines are available which contain a transgene including a minimal promoter driving *GAL4* expression inserted adjacent to endogenous or cryptic tissue-specific enhancer elements in the *Arabidopsis* genome. The transgene also includes *UAS* elements driving *GFP* to localise expression of *GAL4* and verify transactivation of *UAS*. In order to exploit these *GAL4 GFP* enhancer trap lines for tissue-specific luciferase, we generated two constructs. A UAS:JN construct comprising a *UAS* upstream of a fusion of an N-terminal half of LUCIFERASE+ (nLUC+) and the c-Jun bZIP domain of a heterodimer of the AP1 complex. A GW:AC construct comprises a Gateway® cassette upstream of a fusion of a C-terminal half of LUC+ and A-Fos, a leucine zipper domain which interacts with c-Jun (Endo *et al.*, 2014). In principle, when both halves of LUC+ are expressed in the same cell, the stable formation of the AP1 complex will reconstitute the luciferase enzyme and emit bioluminescence in the presence of its substrate, D(+)-Luciferin.

The *GAL4 GFP* enhancer trap system has been adapted to *Arabidopsis* (Haseloff, 1999) and numerous lines have been reported and characterised (Laplaze *et al.*, 2005; Radoeva *et al.*, 2016) and are available from seed stock centres (Table S1). As a proof of concept, we chose four *Arabidopsis* enhancer trap lines with distinct patterns of expression in the leaf. These lines have tissue-specific GFP expression in spongy mesophyll (JR11-2), leaf vasculature (KC274), leaf epidermis (KC464) and guard cells (E1728), as previously shown with confocal laser scanning microscopy (Gardner *et al.*, 2009; Martí *et al.*, 2013). To confirm that these lines can drive transactivated expression of a reporter in a second transgene in the expected tissues, we introduced a *UAS:β-GLUCURONIDASE (GUS)* construct by transformation. For all four *GAL4 GFP* lines, strong GUS activity was consistently detected in the expected tissue or cell types, (Figure 2a). Weak GUS staining was sometimes detected in neighbouring cells, which we interpret as diffusion of the reaction product. The expected GUS patterns were observed in 50/52 T1 seedlings, representing the four lines. This suggests tissue-specific transactivation is robust in these *GAL4 GFP* enhancer trap lines.

In order to further characterise these lines, we used Thermal Asymmetric InterLaced (TAIL) PCR (Liu and Whittier, 1995) to identify the positions of the T-DNA inserts in the genome (Figure 2b). We confirmed the T-DNA in E1728 (guard cell *GAL4 GFP* enhancer trap line) on chromosome 5 (position 26215578) flanked by the coding sequences of a putative chloroplast-targeted Dof zinc finger transcription factor (At5g65590; *STOMATAL CARPENTER 1, SCAP1*) and a L-type lectin

receptor kinase (At5g65600, *LECRK-IX.2*), as previously reported (Gardner *et al.*, 2009). The orientation of the *GAL4 GFP* transgene is in the opposite orientation to both flanking genes (Figure 2b). The T-DNA in KC464 (epidermal *GAL4 GFP* enhancer trap line) was located on chromosome 1 (position 28430296) within the second intron of the gene sequence of a C2H2-like zinc finger protein (At1g75710), 1490 bp downstream of the start codon in the same orientation as the gene. Thus, *GAL4* might be expressed similarly to the protein coding gene (Figure 2b). The T-DNA in KC274 (vascular *GAL4 GFP* enhancer trap line) is located on chromosome 3 (position 19256215), flanked by the coding sequences of a chloroplast-localised sulphate transporter (At3g51895; *SULTR3;1*) and a heat shock transcription factor (At3g51910; *HSFA7A*). The *GAL4 GFP* transgene is 538 bp upstream of At3g51895 and oriented in the same direction (Figure 2b). The T-DNA in JR11-2 (spongy mesophyll *GAL4 GFP* enhancer trap line) is on chromosome 5 (position 5217128), flanked by the coding sequences of a putative member of the pentatricopeptide repeat superfamily (At5g15980) and an NSP-interacting receptor-like kinase (At5g16000; *NIK1*). The *GAL4 GFP* transgene is in the same orientation as both flanking genes, upstream of At5g16000 (Figure 2b).

To validate the use of the selected enhancer trap lines for investigation of circadian rhythms of gene expression, we examined the rhythmic expression of the gene adjacent to each enhancer trap locus using Diurnal, a database of published microarray data sets (Mockler *et al.*, 2007; Figure 2c). The expression of At5g65590 (E1728, guard cell), At1g75710 (KC464, epidermal) or At5g16000 (JR11-2, spongy mesophyll) were not overtly rhythmic in diel (LDHC) or continuous light (LL\_LDHC) conditions. Expression of At3g51895 (KC274, vascular) was rhythmic in both diel and continuous light, peaking at dawn.

Expression of the gene adjacent to the *GAL4 GFP* transgene might not be an indicative marker for the activity of the enhancer. Therefore, we directly measured expression of the *GAL4* transcript by quantitative RT-PCR (qRT-PCR) in the epidermal, vascular and spongy mesophyll lines over a 24 h diel cycle (Figure 3). Consistent with the Diurnal data (Figure 2c), diel rhythms of *GAL4* transcript level were not detected in the spongy mesophyll or epidermal lines. Transcript levels of *GAL4* peaked at zeitgeber time (ZT) 0 in the vascular line, although the amplitude was substantially lower than circadian clock genes *CIRCADIAN CLOCK ASSOCIATED 1 (CCA1)* and *TIMING OF CAB2 1 (TOC1)* (Figure 3). The diel oscillation of *GAL4* in this enhancer trap line might alter the rhythms of the reconstituted luciferase in these tissues. On the other hand, the relatively low amplitude rhythm of the enhancer might not be sufficient to substantively impact regulation of the UAS in the context of highly expressed circadian clock reporters. In either case, examination of rhythmic expression of *GAL4* in each enhancer line is necessary to interpret estimates of circadian rhythms with this split luciferase system.

The ETSLA system requires the introduction of two transgenes into the *GAL4 GFP* enhancer trap lines. We reasoned that best strategy was to co-transform the UAS:JN and promoter:AC construct into wild-type *A. thaliana* by floral dip and then cross the double transformants with each enhancer trap line and measure luminescence in F1 and subsequent generations. The advantage of this strategy is that differences between luciferase signal can be confidently assigned to the enhancer trap by controlling for position effects of the new transgenes. We also used an alternative strategy of transforming the UAS:JN construct into each enhancer trap line and then crossing these double transgenics to each promoter:AC transgenic. The latter strategy has the advantage of versatility of the system for new promoters of interest.

To test the application of the ETSLA system to measure circadian rhythms in Arabidopsis seedlings, we used the GW:AC vector to generate constructs for three core circadian oscillator genes with distinct phases in the morning (*CCA1*), afternoon (*PSEUDO RESPONSE REGULATOR 7; PRR7*) and evening (*TOC1*) and an evening-phased circadian output gene (*COLD, CIRCADIAN RHYTHM AND RNA BINDING 2; CCR2*). The promoter:AC and UAS:JN constructs were introduced into the enhancer trap lines by one or both of the alternative strategies described above (Table S2). We identified populations harbouring all three transgenes for the vascular and mesophyll enhancer trap lines and detected luminescence in all lines. We first confirmed that the presence of all three transgenes is both necessary and sufficient to produce luciferase luminescence. We did not detect luminescence signal above background levels in Arabidopsis seedlings containing any two of a promoter:AC, UAS:JN or a *GAL4 GFP* transgene. Clear signal was only detected when all three transgenes were present (Figure 4a). Luminescence imaging of the *TOC1* vascular ETSLA lines, carrying all three transgenes, indicated a clear vascular pattern of luminescence signal in leaves (Figure 4b). Together, these confirm that the split luciferase enzyme can be effectively reconstituted using the *GAL4 GFP* enhancer trap lines to produce tissue-specific luminescence in Arabidopsis seedlings.

#### *Tissue-specific features of circadian oscillator gene expression*

To measure circadian rhythms in the ETSLA lines we imaged luminescence in multiple populations (Table S2) harbouring all three transgenes in continuous light and compared them to promoter:*LUC* lines reporting whole-seedling promoter activity (Figure 5). Robust circadian rhythms were detected for all promoters with a period ranging from 21-28 h (mean period  $22.3 \pm 1.3$  h; mean relative amplitude error  $0.28 \pm 0.15$ ; Table S2). For the *CCA1* promoter, we could not detect a difference in circadian period or phase between the vascular or mesophyll ETSLA lines and *CCA1p:LUC* control (Figure 5a). This suggests circadian rhythms of *CCA1* expression are similar in vascular and mesophyll tissues, as previously reported (Endo *et al.*, 2014).

*PRR7p:LUC* activity comprises two peaks in diel cycles (Figure 5b); a light-activated peak at dawn followed by a circadian peak in the afternoon. Rhythms of *PRR7* promoter were distinct in mesophyll and vascular tissues. Circadian period was significantly longer in both tissue types compared to whole-seedling *PRR7p:LUC* activity, particularly in the vascular ETSLA lines. The circadian phase of the *PRR7* promoter was significantly advanced by about 9 h in the vascular line compared to *PRR7p:LUC*, suggesting distinct oscillator behaviour between these cell types. Interestingly, the earlier peak of *PRR7* in the vascular line coincides with the phase of the light-activated peak in *PRR7p:LUC*, so might be due to increased light-sensitivity of these cells.

The period of *TOC1* promoter activity was similar in the mesophyll ETSLA lines compared to total *TOC1p:LUC* with a small, but significant, phase delay (1.3 h; Figure 5c). By contrast, the period of *TOC1* promoter activity was significantly longer in vascular lines compared to *TOC1p:LUC* and the phase was dramatically advanced, similar to *PRR7*. Differences in circadian rhythms of *TOC1* promoter have previously been reported when driven ubiquitously or in phloem companion cells from the *SUCROSE-PROTON SYMPORTER 2 (SUC2)* promoter (Endo *et al.*, 2014), so we directly compared rhythms in *SUC2p/TOC1p* TSLA with the vascular ETSLA lines (Figure 5c). We did not detect a significant difference in circadian period or phase between the *SUC2p/TOC1p* TSLA lines compared to *TOC1p:LUC* or the *TOC1* mesophyll ETSLA lines in our experiments. The differences in luciferase rhythms between the *SUC2p/TOC1p* TSLA and the *TOC1* vascular ETSLA lines might be due to differences in tissue-specificity of these two lines. The *SUC2* promoter is specifically active in phloem companion cells (Truernit and Sauer, 1995; Schulze *et al.*, 2003), whereas we detected broad expression throughout leaf vascular bundles from the vascular enhancer (Figure 2a).

We considered whether the earlier phase in the vascular ETSLA lines for both *TOC1* and *PRR7* might be caused by the weak dawn phase of the vascular enhancer (Figures 2b, c). However, we think the phase reported by the ETSLA lines is a true reflection of the phase *TOC1* and *PRR7* promoters in this tissue because the phase of the *CCR2* promoter in the vascular ETSLA lines was not shifted compared to *CCR2p:LUC*, which is phased in the evening similar to *TOC1* (Figure 5d). Luciferase activity in the *CCR2* mesophyll ETSLA lines was poorly rhythmic (Figure 5d). This might reflect expression of this circadian output in this tissue or could be due to silencing of any one of the three transgenes. The latter is a potential pitfall of introducing multiple transgenes, but this has not been a barrier for the majority of ETSLA lines. In summary, these data confirm the utility of the ETSLA system to study tissue-specific circadian rhythms and confirm distinct circadian oscillator behaviour in different tissue types.

Having observed striking phase difference of the *TOC1* promoter in the vascular ETSLA lines, we further examined the expression of transcripts in these lines by qRT-PCR (Figure 6). We measured



transcripts for oscillator genes and each of the three transgenes in shoots of F2 plants of the *TOC1* vascular ETSLA lines grown for 24 h in continuous light (Figure 6a). Robust rhythms of endogenous *CCA1* and *TOC1* expression were phased in the morning and evening, respectively, as expected. Robust, rhythmic expression was also detected for the *TOC1p:AC* transgene in the same phase as *TOC1*, confirming that the transgene is correctly expressed. Expression of *GAL4* and the transactivated *UAS:JN* transgene were similar in these plants to that observed for *GAL4* in the parental vascular enhancer trap line (Figure 3) with a low amplitude rhythm phased in the subjective morning. We also measured transcripts in these ETSLA F2 plants at ZT5 and ZT13 in a diel growth cycle (Figure 6b). We detected similar expression of the *TOC1p:AC* transgene to *TOC1* and low levels of expression of the transactivated *UAS:JN* transgene. Thus, in both diel and continuous light conditions, the relative expression of the dawn-phased *nLUC* transcript is substantially lower than the expression of the evening-phased *cLUC* transcript in the *TOC1* vascular ETSLA lines. This suggests that the phase shift of *TOC1* promoter activity in these lines is a true reflection of the phase of *TOC1* promoter activity in vascular tissue.

#### *Tissue-specific expression of carbon starvation markers*

Sugar signalling and metabolism are closely associated with the circadian clock (Blasing *et al.*, 2005; Graf *et al.*, 2010; Dalchau *et al.*, 2011; Haydon *et al.*, 2013; Haydon *et al.*, 2017) but little is known about tissue-specificity of sugar signalling networks. We generated promoter:AC constructs for *DARK INDUCIBLE 6 (DIN6)* and *SENESCENCE 5 (SEN5)*, two transcriptional markers of Snf1-related protein kinase 1 (SnRK1; Rodrigues *et al.*, 2013), which is a signalling hub for carbon starvation (Baena-Gonzalez *et al.*, 2007) and modulator of circadian rhythms in Arabidopsis (Frank *et al.*, 2018). Robust circadian rhythms of luminescence were detected in both *DIN6p:LUC* and *SEN5p:LUC* transgenic lines (Figure 7), as expected (Frank *et al.*, 2018). No significant difference in circadian period or phase was detected between *DIN6p:LUC* and the *DIN6* vascular ETSLA line (Figure 7a). This suggests that, similar to *CCR2* (Figure 5d), morning phasing of this circadian output is not apparent in vascular tissue. For the *SEN5* promoter, we were able to isolate ETSLA lines for mesophyll, vasculature and guard cells (Figure 7b). Robust luciferase rhythms were detected in the *SEN5* guard cell ETSLA line, suggesting this system is compatible with detecting luciferase expression in potentially very small pools of cells. No difference in circadian period was detected between any ETSLA lines and the *SEN5p:LUC* control, but significantly earlier phase was detected for the vascular line, similar to *TOC1* and *PRR7*. Thus, there might be heterogeneity in distinct networks of circadian outputs.

## Discussion

By building and verifying constructs for a split luciferase system that is compatible with *GAL4* enhancer trap lines, we have established the tools and demonstrated utility of a versatile transgenic toolset for spatiotemporal measurement of gene expression in Arabidopsis. We have demonstrated heterogeneity of gene expression dynamics of core circadian clock gene promoters and circadian-regulated outputs. We have shown significant differences between the period and/or phase of circadian rhythms in vascular tissue compared to leaf mesophyll and whole-seedling rhythms for promoters of *TOC1*, *PRR7* and *SEN5*, but not *CCA1*, *CCR2* or *DIN6*. This indicates that although there is spatial heterogeneity of circadian rhythms in Arabidopsis leaves, it is not representative of all circadian oscillator components or outputs, suggesting the existence of distinct circadian networks in particular cell types.

We have used the ETSLA system to measure expression of circadian-regulated promoters because the spatial heterogeneity and organisation of circadian oscillators in plant cells is emerging as a fascinating area of research (Endo *et al.*, 2014; Takahashi *et al.*, 2015; Gould *et al.*, 2018; Greenwood *et al.* 2019). To ensure each enhancer trap line was suitable for this purpose, we measured circadian rhythms of the *GAL4* transcript, driven by the enhancer. This validation could be similarly achieved by introducing a *UAS:LUC* transgene. The tools we have generated are applicable to explore tissue-specific dynamics of gene expression for any stimuli of interest. The particular advantages of the ETSLA system are that detection of luminescence is non-destructive and can be measured in living plants growing in controlled conditions. Luminescence detection is not restricted by position of cell types within the tissue and has sufficient sensitivity to measure relatively small populations of cells. We have successfully detected tissue-specific gene expression using enhancer trap lines for vasculature, mesophyll and guard cells, but the system is compatible with numerous published lines (Laplaze *et al.*, 2005; Gardner *et al.*, 2009; Ckurshumova *et al.*, 2009; Radoeva *et al.*, 2016; Table S1) among hundreds available from seed stock centres. Once the lines have been generated, luminescence experiments can be easily performed. Thus, the ETSLA system is ideally suited to explore effects of environmental conditions or pharmacological treatments on gene expression. For circadian clock research, these approaches could provide insight into communication between oscillators in different cells.

The ETSLA system can be easily utilised by generating a single construct using the Gateway®-compatible GW:AC plasmid. This can be used to introduce any promoter of interest and also may be suitable for translational fusions to the A-FOS:cLUC fragment. Transformants can be crossed into any *GAL4 GFP* enhancer trap line carrying the *UAS:JN* transgene, which we have obtained for four lines in this study. This strategy of independent AC and JN transgenes allows for control of

transgene position effects. However, introducing the *UAS:JN* sequence into the *GW:AC* plasmid might be worthwhile improvement to the ETSLA system.

We did not identify epidermal ETSLA lines with detectable luminescence in this study. Notwithstanding that we could show effective tissue-specific expression of a *UAS:GUS* transgene (Figure 2a) and previously a *UAS:AEQUORIN* (Martí *et al.*, 2013) in the epidermal enhancer trap line, the lack of signal in the ETSLA lines might be due to large vacuoles in epidermal cells affecting luciferase signal or low promoter activity in these cells of the particular genes investigated. Epidermal *GAL4 GFP* lines with a *UAS:JN* transgene identified in this study could be used to test other promoter:AC constructs.

Our observation of distinct circadian rhythms in vascular tissue is consistent with a previous study (Endo *et al.*, 2014). A *SUC2p/TOC1p* TSLA line, which drives expression specifically in phloem companion cells was reported with a later phase compared to a *35Sp/TOC1p* TSLA line. We did not detect a significant difference in circadian rhythms of the *SUC2p/TOC1p* TSLA line in our experiments compared to *TOC1p:LUC* or *TOC1* mesophyll ETSLA seedlings. This may be due to the different control line or inclusion of sucrose in the media, which alters circadian rhythms in *Arabidopsis* (Haydon *et al.*, 2013; Haydon *et al.*, 2017) and activity of the *SUC2* promoter (Truernit and Sauer, 1995). By contrast, we observed both significantly lengthened period and phase advance of *TOC1* promoter activity in vascular ETSLA lines, with similar effects for *PRR7* and *CCR2* promoters. The very different luciferase rhythms in *TOC1* vascular ETSLA lines compared to the *SUC2p/TOC1p* TSLA line is likely because of the different expression pattern of *GAL4* and *UAS:GUS* in the vascular enhancer trap line (KC274), for which we detected a much broader pattern of expression throughout vascular bundles compared to *SUC2* promoter activity specifically in phloem companion cells. Thus, there appears to be spatial heterogeneity of circadian rhythms even within vascular tissues.

The tissue-specific features of circadian oscillators might be important for regulating distinct physiological or developmental outputs. Expression of *CCA1* from a range of tissue-specific promoters resulted in different effects on photoperiodic flowering (Shimizu *et al.*, 2015). Expression of *CCA1* in phloem companion cells from the *SUC2* promoter delayed flowering in long days, but not when *CCA1* was expressed from *IRREGULAR XYLEM 3 (IRX3)* or *HOMEBOX GENE 8 (HB8)* promoters which are specific to xylem and procambium, respectively (Shimizu *et al.*, 2015). While these results are consistent with a specific role for the oscillator in companion cells for regulating flowering, they could also be explained by relatively high expression of *SUC2*, compared to *IRX3* and *HB8*, or different phases of the three promoters (Mockler *et al.*, 2007). Indeed, our characterisation of the circadian expression of *GAL4* in each enhancer trap line demonstrates the importance of considering the expression dynamics of any chosen tissue-specific promoter.

The differences in gene expression dynamics of circadian clock genes, which we detected in different ETSLA lines could be due to differences in light sensitivity of particular cell types. For example, the earlier light-activated peak of *PRR7p:LUC* appeared more pronounced in the vascular ETSLA line compared to whole-seedling rhythms. It has been suggested that light-piping through vascular tissue might contribute to maintain circadian rhythms in *Arabidopsis* roots (Bordage *et al.*, 2016). Vascular cells might be more sensitive to light signals, or transmission of light through vasculature might be more efficient than mesophyll. The ETSLA system could be an effective tool to explore these dynamics in a wider range of vascular cell types, since several vascular *GAL4 GFP* enhancer trap lines are available (Table S1).

## **Conclusion**

We have adapted a split luciferase system to be compatible with available collections of enhancer trap lines and Gateway®-compatible vectors to provide a versatile system for monitoring dynamic gene expression in specific tissues or cell types. We have validated a small selection of enhancer trap lines for leaf expression and confirmed their suitability to measure tissue-specific circadian rhythms. We have corroborated previous data suggesting heterogeneity in circadian behaviour between leaf mesophyll and vascular tissues and expanded the tool set to investigate this behaviour. We hope this tool will provide a flexible resource to advance research to explore spatial heterogeneity in gene expression and identify sensitivity of particular tissues to various environmental stimuli and endogenous signals in intact, living plants.

## Experimental procedures

### *Plasmid constructs*

TOC1p:AC and CCA1p:AC plasmids have been described (Endo *et al.*, 2014). To generate CCR2p:AC, a 2024 bp promoter fragment was amplified from gDNA of Columbia-0 (Col-0) by PCR with primers containing HindIII sites and ligated into the TOC1p:AC plasmid in place of the *TOC1p* sequence. The GW:AC plasmid was made by PCR amplification of a 544 bp *A-Fos:nLUC* (AC) fragment from TOC1p:AC using primers containing *Xba*I and *Spe*I sites and ligated into pEarlyGate301 (Earley *et al.*, 2006). For the *PRR7p:AC*, *SEN5p:AC* and *DIN6p:AC*, a 1020 bp *PRR7* promoter, 1666 bp *SEN5* promoter and 1017 bp *DIN6* were amplified by PCR from Col-0 gDNA and cloned into pENTR/D-TOPO (Invitrogen) and recombined into the with GW:AC plasmid. The *SEN5* promoter was also cloned into pEarlyGate301-LUC+, comprised of a LUC+ fragment amplified from *CCR2p:LUC+* seedlings (Haydon *et al.*, 2013) and ligated into *Xba*I sites of pEarlyGate301 (Earley *et al.*, 2006).

The UAS:JN plasmid was generated by PCR amplification of a 656 bp c-Jun:cLUC (JN) fragment from gDNA of TOC1:AC / SUC2:JN seedlings (Endo *et al.*, 2014) with primers containing *Bam*HI and *Sac*I restriction sites. The JN sequence was ligated into pBINYFPAEQ plasmid (Kiegle *et al.*, 2000) in place of the YFP:AEQ sequence, downstream of the UAS. The UAS:GUS plasmid has been described previously (Møller *et al.* 2009).

All primers are listed in Table S3.

### *Plant materials*

Stable transgenic lines for *CCA1p:LUC+*, *TOC1p:LUC+*, *PRR7p:LUC+*, *CCR2p:LUC+*, *DIN6p:LUC+* and *TOC1p:AC / SUC2p:JN* are in Col-0 and have been used previously (Haydon *et al.*, 2013; Endo *et al.*, 2014; Frank *et al.*, 2018). The *GAL4 GFP* enhancer trap lines E1728, JR11-2, KC274 and KC464 are in C24 and have been described (Gardner *et al.*, 2009; Martí *et al.*, 2013).

*TOC1p:AC*, *PRR7p:AC*, *CCA1p:AC*, *CCR2p:AC*, *SEN5p:AC* and *DIN6:AC* were transformed, or co-transformed with *UAS:JN*, into Col-0 by floral dip (Clough and Bent, 1998). *UAS:JN* was also transformed into each of the *GAL4 GFP* enhancer trap lines. Homozygous T3 populations of plants harbouring both the *promoter:AC* and *UAS:JN* transgenes were crossed to *GAL4 GFP* lines. As an alternative approach, *UAS:JN* transformants were identified for all four *GAL4 GFP* enhancer trap lines and T1-T2 populations of *promoter:AC* transformants were crossed to T1 populations of

*UAS:JN* transformants. Experiments were performed with F1 or F2 populations which would be heterozygous or segregating for the three dominant transgenes, respectively.

### *Luminescence experiments*

Seeds were surface sterilised with a solution of 20 % (v/v) bleach, 0.02 % (v/v) Triton X-100 and washed three times with sterile deionised water. Seeds were sown in clusters of five to twenty on modified Hoagland media (Haydon *et al.*, 2012), solidified with 0.8 % agar type M. Plates were chilled for 2 days at 4°C and grown in 12 h light, 12 h dark (LD) cycles at 20 °C. Light was supplied from red (660 nm), green (550 nm), blue (450 nm) and far-red (730 nm) LED array (HiPoint) at 50  $\mu\text{mol m}^{-2} \text{s}^{-1}$ . Ten to 14 d old seedlings were treated twice with a topical application of 1 mM D-luciferin, K<sup>+</sup> salt at least 24 h prior to photon counting. Luminescence was measured for 600 s, following a 2 min delay to decay chlorophyll fluorescence (Gould *et al.* 2009) at 1 h intervals for 48 h in LD and 120 h of continuous light in a HRPCS2 (Photek) with light supplied from red (660 nm) and blue (470 nm) LEDs at 50  $\mu\text{mol m}^{-2} \text{s}^{-1}$ . Luminescence for each cluster was normalised to average counts across the time series. Circadian period and circadian phase (corrected for circadian period in free-running conditions) estimates were performed on raw luminescence data between 24 and 120 h in continuous light using fast Fourier Transform-nonlinear least squares (FFT-NLLS) analysis, using BioDare2 (<https://biodare2.ed.ac.uk/>) (Zielinski *et al.*, 2014). Spatial imaging of luminescence in ETSLA lines (Figure 4) used a NightShade LB 985 Plant Imaging System (Berthold).

### *Thermal Asymmetric InterLaced (TAIL) PCR*

The genomic locations of the *GAL4 GFP* T-DNAs were determined by TAIL PCR, essentially as described (Liu and Whittier, 1995), using nested specific primers complementary to the right or left T-DNA borders and a degenerate primer (Table S3), as described (Gardner *et al.*, 2009). The products of the tertiary reaction were cloned and sequenced to identify the flanking genomic region(s) of the T-DNA.

### *Quantitative RT-PCR*

Shoots of 14 d old seedlings were snap frozen in liquid N. Total RNA was extracted from frozen tissue using Isolate II Plant RNA Kit (Bioline) with on-column DNaseI treatment. cDNA was prepared from 0.5  $\mu\text{g}$  RNA with Tetro cDNA Synthesis Kit (Bioline) using oligo-dT primer. Technical replicates of gene-specific products were amplified with primers in Table S2 in 10  $\mu\text{L}$  reactions using SensiFAST SYBR no-ROX kit (Bioline) on a CFX96 Thermocycler (BioRad). Transcript levels were calculated from C<sub>t</sub> values, incorporating PCR efficiencies calculated with LinRegPCR (Ruijter *et al.*, 2009), relative to the geometric mean of two reference genes

*ISOPENTENYL PYROPHOSPHATE: DIMETHYLALLYL PYROPHOSPHATE ISOMERASE 2 (IPP2)* and *PROTEIN PHOSPHATASE 2A SUBUNIT A3 (PP2AA3)* (Vandesompele *et al.*, 2002).

*$\beta$ -glucuronidase (GUS) stains*

T1 seedlings of *GAL4 GFP* enhancer trap lines transformed with UAS:GUS were GUS-stained overnight as previously (Haydon *et al.* 2007) and imaged with a SMZ800 stereomicroscope (Nikon). For leaf sections, seedlings were fixed in a formaldehyde-acetic acid-ethanol (3.7 %-5 %-50 %) mix, dehydrated in a series of an increasingly concentrated ethanol solution and imbibed in series of histoclear. Tissue was infiltrated with wax (Paraplast plus) and subsequently sectioned (8  $\mu$ m). Sections were imaged with a BX60 microscope (Olympus) using DIC optics.



## **Acknowledgements**

We thank Dr. Motomu Endo (Kyoto University) for providing seed of the TOC1:AC/SUC2:JN TSLA line and plasmids for TOC1p:AC and CCA1p:AC, Prof. Matt Gilliam (University of Adelaide) for providing the UAS:GUS plasmid, Ms. Heather Eastmond (University of York) and Mr. Matthew Stancombe (University of Cambridge) for technical assistance and Dr. Fabian Vaistij (University of York) for helpful advice. Funding was provided by the BBSRC (BB/L021188/1), The Royal Society (RG150144) and the University of Melbourne through the Faculty of Science Researcher Grant Support Scheme. The authors declare there are no conflicts of interest.

## Table titles and Figure legends

**Figure 1.** Components of the enhancer trap tissue-specific split luciferase assay system. In the *GAL4 GFP* enhancer trap lines, expression of *GAL4* is driven by a minimal promoter in the transgene and a tissue-specific enhancer in the genome. *GAL4*, a yeast transcriptional activator, binds to upstream activation sequences (*UAS*) to produce tissue-specific expression of GFP, which is encoded by the same transgene. The split luciferase system requires introduction of two transgenes. In one, *UAS* is upstream of a sequence coding a fusion product of an N-terminal region of luciferase and a c-Jun subunit of the AP1 complex. In the second, a promoter of interest is inserted between *att* sites by Gateway® cloning upstream of a sequence for a fusion of the C-terminal region of luciferase and an A-Fos subunit of the AP1 complex. Co-expression of all three transgenes in a cell (for example, in leaf vasculature) allows reconstitution of a functional luciferase enzyme, facilitated by the stable interaction of the AP1 complex subunits, generating tissue-specific luminescence (yellow line). Cells in which the tissue-specific enhancer is not activated express only the C-terminal half of luciferase (blue line) and do not produce luminescence.

**Figure 2.** Characterisation of *GAL4 GFP* enhancer trap lines used in this study.

(a) GUS stains of 20 d old T1 transformants of *UAS:GUS* in *GAL4 GFP* enhancer trap lines in guard cells (E1728), leaf epidermis (KC464), vasculature (KC274) and spongy mesophyll (JR11-2). Leaf cross sections are shown for the epidermal, vascular and mesophyll lines (right). Bars represent 1 mm (left, middle) or 100 µm (right). (b) Genomic location and orientation of the *GAL4 GFP* T-DNAs. Flanking protein coding genes are shown. Arrows indicate direction of transcription. (c) Expression of transcripts adjacent to each *GAL4 GFP* T-DNA in diel (LDHC) or continuous light (LL\_LDHC) conditions. Data were obtained from diurnal.mocklerlab.org (Mockler *et al.*, 2007).

**Figure 3.** Transcript levels in *GAL4 GFP* enhancer trap lines in diel conditions.

Transcript levels of *TOC1*, *CCA1* and *GAL4*, relative to *IPP2* and *PP2AA3*, in 10-14 d old enhancer trap line seedlings growing in light-dark cycles. Values are means ± SD, n=3.

**Figure 4.** Tissue-specific luminescence using ETSLA.

(a) Luciferase luminescence in transgenic seedlings containing combinations of a *CCA1p:AC* (*cLUC*), *TOC1p:AC* and *UAS:JN* (*nLUC*) transgenes transformed into wild-type (Col-0) or *GAL4 GFP* enhancer trap lines. Data are represented as Min Max box plots, n=4. Asterisks indicated statistical difference from non-transformed wild-type by two-tailed *t*-test with Bonferroni corrections ( $P < 0.01$ ). (b) Luminescence image overlaid on a bright-field image of 15 d old seedlings containing *TOC1p:AC* and *UAS:JN* transgenes in the vascular *GAL4 GFP* enhancer trap line (KC274). Bar represents 10 mm. False colour scale represents counts per second (cps).

**Figure 5.** Tissue-specific circadian clock promoter activity using ETSLA.

Normalised luminescence, period and phase estimates of luciferase activity in 10-14 d old seedlings in continuous light for (a) *CCA1*, (b) *PRR7*, (c) *TOC1* and (d) *CCR2* promoters. ETSLA lines for vascular and mesophyll expression are shown, compared to the promoter:LUC control for each gene and the *SUC2*-driven TSLA line for *TOC1*. Luminescence values are means  $\pm$  SEM, n=4-8. Period and phase estimates are represented as Min Max box plots. Statistical differences from the promoter:LUC control were determined by One-way ANOVA with Tukey's post-hoc tests. Different letters indicate significant differences between samples ( $P < 0.05$ ).

**Figure 6.** Transcript levels in the *TOC1* vascular ETSLA line.

Transcript levels of *TOC1*, *CCA1*, *GAL4*, *nLUC* and *cLUC*, relative to *IPP1* and *PP2AA3* in 10-14 d old *TOC1* vascular ETSLA line seedlings growing in (a) continuous light or (b) diel conditions. Values are means  $\pm$  SD, n=3.

**Figure 7.** Tissue-specific carbon starvation promoter activity using ETSLA.

Normalised luminescence, period and phase estimates of luciferase activity in 10-14 d old seedlings in continuous light. (a) *DIN6* vascular ETSLA line and (b) *SEN5* vascular, mesophyll and guard cell ETSLA lines are shown, compared to the promoter:LUC control for each gene. Luminescence values are means  $\pm$  SEM, n=4. Period and phase estimates are represented as Min Max box plots. Statistical differences from the promoter:LUC control were determined by One-way ANOVA with Tukey's post-hoc tests. Different letters indicate significant differences between samples ( $P < 0.05$ ).

**Table S1.** List of published GAL4 enhancer trap lines compatible with the ETSLA system.

**Table S2.** Summary of transgenic lines used in this study.

**Table S3.** Sequences of primers used in this study.

## References

- Asano, T., Masumura, T., Kusano, H., Kikuchi, S., Kurita, A., Shimada, H. and Kadowaki, K.-I.** (2002) Construction of a specialized cDNA library from plant cells isolated by laser capture microdissection: toward comprehensive analysis of the genes expressed in the rice phloem. *Plant J.*, **32**, 401–408.
- Baena-Gonzalez, E., Rolland, F., Thevelein, J.M. and Sheen, J.** (2007) A central integrator of transcription networks in plant stress and energy signalling. *Nature*, **448**, 938–942.
- Birnbaum, K., Shasha, D.E., Wang, J.Y., Jung, J.W., Lambert, G.M., Galbraith, D.W. and Benfey, P.N.** (2003) A gene expression map of the Arabidopsis root. *Science*, **302**, 1956–1960.
- Blasing, O.E., Gibon, Y., Gunther, M., et al.** (2005) Sugars and circadian regulation make major contributions to the global regulation of diurnal gene expression in Arabidopsis. *Plant Cell*, **17**, 3257–3281.
- Bonner, R.F., Emmert-Buck, M., Cole, K., Pohida, T., Chuaqui, R., Goldstein, S. and Liotta, L.A.** (1997) Laser capture microdissection: molecular analysis of tissue. *Science*, **278**, 1481–1483.
- Bordage, S., Sullivan, S., Laird, J., Millar, A.J. and Nimmo, H.G.** (2016) Organ specificity in the plant circadian system is explained by different light inputs to the shoot and root clocks. *New Phytol.*, **212**, 136–149.
- Brady, S.M., Song, S., Dhugga, K.S., Rafalski, J.A. and Benfey, P.N.** (2007) Combining expression and comparative evolutionary analysis. The COBRA gene family. *Plant Physiol.*, **143**, 172–187.
- Ckurshumova, W., Koizumi, K., Chatfield, S.P., Sanchez-Buelna, S.U., Gangaeva, A.E., McKenzie, R. and Berleth, T.** (2009) Tissue-specific GAL4 expression patterns as a resource enabling targeted gene expression, cell type-specific transcript profiling and gene function characterization in the Arabidopsis vascular system. *Plant Cell Physiol.*, **50**, 141–150.
- Clough, S.J. and Bent, A.F.** (1998) Floral dip: A simplified method for Agrobacterium-mediated transformation of Arabidopsis thaliana. *Plant J.*, **16**, 735–743.
- Coker, T.L.R., Cevik, V., Beynon, J.L. and Gifford, M.L.** (2015) Spatial dissection of the Arabidopsis thaliana transcriptional response to downy mildew using Fluorescence Activated Cell Sorting. *Front. Plant Sci.*, **6**, 1–13.
- Dalchau, N., Baek, S.J., Briggs, H.M., et al.** (2011) The circadian oscillator gene GIGANTEA mediates a long-term response of the Arabidopsis thaliana circadian clock to sucrose. *Proc. Natl. Acad. Sci. U. S. A.*, **108**, 5104–5109.
- Deal, R.B. and Henikoff, S.** (2011) The INTACT method for cell type-specific gene expression and chromatin profiling in Arabidopsis thaliana. *Nat. Protoc.*, **6**, 56–68.
- Denyer, T., Ma, X., Klesen, S., Scacchi, E., Nieselt, K. and Timmermans, M.C.P.** (2019) Spatiotemporal Developmental Trajectories in the Arabidopsis Root Revealed Using High-

- Throughput Single-Cell RNA Sequencing. *Dev. Cell*, **48**, 840–852.
- Dinneny, J.R., Long, T.A., Wang, J.Y., et al.** (2008) Cell identity mediates the response of Arabidopsis roots to abiotic stress. *Science*, **320**, 942–945.
- Dodd, A.N., Jakobsen, M.K., Baker, A.J., et al.** (2006) Time of day modulates low-temperature Ca<sup>2+</sup> signals in Arabidopsis. *Plant J.*, **48**, 962–973.
- Earley, K.W., Haag, J.R., Pontes, O., Opper, K., Juehne, T., Song, K. and Pikaard, C.S.** (2006) Gateway-compatible vectors for plant functional genomics and proteomics. *Plant J.*, **45**, 616–629.
- Efroni, I. and Birnbaum, K.D.** (2016) The potential of single-cell profiling in plants. *Genome Biol.*, **17**, 1–8.
- Emmert-Buck, M.R., Bonner, R.F., Smith, P.D., Chuaqui, R.F., Zhuang, Z., Goldstein, S.R., Weiss, R.A. and Liotta, L.A.** (1996) Laser capture microdissection. *Science*, **274**, 998–1001.
- Endo, M., Shimizu, H., Nohales, M.A., Araki, T. and Kay, S.A.** (2014) Tissue-specific clocks in Arabidopsis show asymmetric coupling. *Nature*, **515**, 419–422.
- Frank, A., Matioli, C.C., Viana, A.J.C., et al.** (2018) Circadian Entrainment in Arabidopsis by the Sugar-Responsive Transcription Factor bZIP63. *Curr. Biol.*, **28**, 2597–2606.
- Gan, Y., Bernreiter, A., Filleur, S., Abram, B. and Forde, B.G.** (2012) Overexpressing the ANR1 MADS-box gene in transgenic plants provides new insights into its role in the nitrate regulation of root development. *Plant Cell Physiol.*, **53**, 1003–1016.
- Gardner, M.J., Baker, A.J., Assie, J.-M.M., Poethig, R.S., Haseloff, J.P. and Webb, A.A.R.** (2009) GAL4 GFP enhancer trap lines for analysis of stomatal guard cell development and gene expression. *J. Exp. Bot.*, **60**, 213–226.
- Gould, P.D., Diaz, P., Hogben, C., Kusakina, J., Salem, R., Hartwell, J. and Hall, A.** (2009), Delayed fluorescence as a universal tool for the measurement of circadian rhythms in higher plants. *Plant J.*, **58**, 893-901.
- Gould, P.D., Domijan, M., Greenwood, M., Tokuda, I.T., Rees, H., Kozma-Bognar, L., Hall, A.J. and Locke, J.C.** (2018) Coordination of robust single cell rhythms in the Arabidopsis circadian clock via spatial waves of gene expression. *Elife*, **7**, 1–20.
- Greenwood M., Domijan M, Gould P.D., Hall A.J.W. and Locke J.C.W.** (2019) Coordinated circadian timing through the integration of local inputs in *Arabidopsis thaliana*. *PLOS Biology* **17**(8): e3000407. <https://doi.org/10.1371/journal.pbio.3000407>
- Graf, A., Schlereth, A., Stitt, M. and Smith, A.M.** (2010) Circadian control of carbohydrate availability for growth in Arabidopsis plants at night. *Proc. Natl. Acad. Sci. U. S. A.*, **107**, 9458–9463.
- Grønlund, J.T., Eyres, A., Kumar, S., Buchanan-Wollaston, V. and Gifford, M.L.** (2012) Cell specific analysis of Arabidopsis leaves using fluorescence activated cell sorting. *J. Vis. Exp.*, **68**, 1–6.
- Haseloff, J.** (1999) GFP variants for multispectral imaging of living cells. *Methods Cell Biol.*, **58**,

139–151.

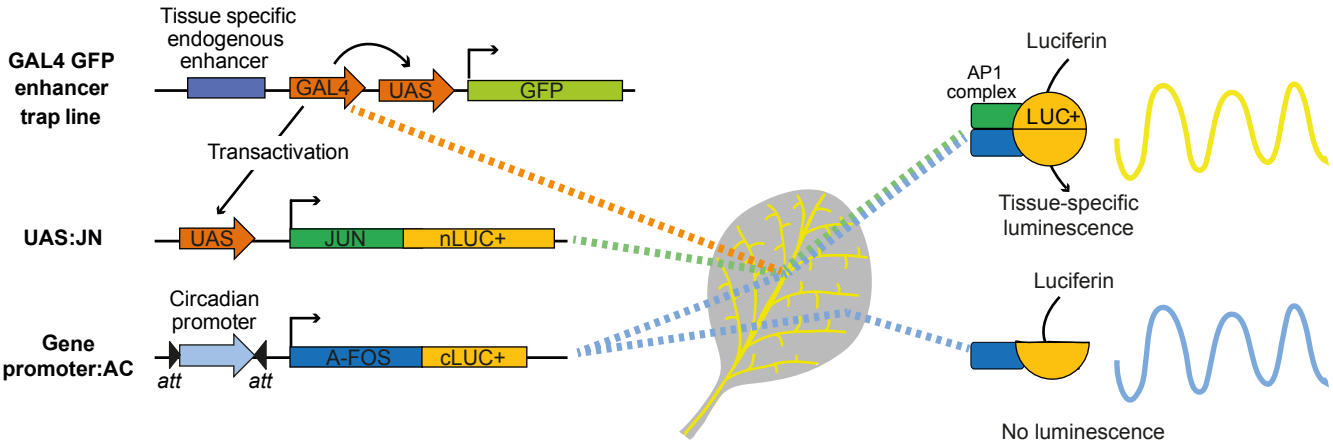
- Haydon, M.J. and Cobbett, C.S.** (2007) A novel major facilitator superfamily protein at the tonoplast influences zinc tolerance and accumulation in *Arabidopsis*. *Plant Physiol.*, **143**, 1705–1719.
- Haydon, M.J., Kawachi, M., Wirtz, M., Hillmer, S., Hell, R. and Kramer, U.** (2012) Vacuolar nicotianamine has critical and distinct roles under iron deficiency and for zinc sequestration in *Arabidopsis*. *Plant Cell*, **24**, 724–737.
- Haydon, M.J., Li, X. and Ting, M.K.-Y.** (2019) Temporal control of plant-environment interactions by the circadian clock. *Annu. Plant Rev.*, **2**, 1–32.
- Haydon, M.J., Mielczarek, O., Frank, A., Roman, A. and Webb, A.A.R.** (2017) Sucrose and Ethylene Signaling Interact to Modulate the Circadian Clock. *Plant Physiol.*, **175**, 947–958.
- Haydon, M.J., Mielczarek, O., Robertson, F.C., Hubbard, K.E. and Webb, A.A.R.R.** (2013) Photosynthetic entrainment of the *Arabidopsis thaliana* circadian clock. *Nature*, **502**, 689–692.
- James, A.B., Monreal, J.A., Nimmo, G.A., Kelly, C.L., Herzyk, P., Jenkins, G.I. and Nimmo, H.G.** (2008) The Circadian Clock in *Arabidopsis* Roots Is a Simplified Slave Version of the Clock in Shoots. *Science*, **322**, 1832–1835.
- Jean-Baptiste, K., McFaline-Figueroa, J.L., Alexandre, C.M., et al.** (2019) Dynamics of Gene Expression in Single Root Cells of *Arabidopsis thaliana*. *Plant Cell*, **31**, 993–1011.
- Jia, H., Look, B. Van, Liao, M., Verbelen, J.-P. and Vissenberg, K.** (2007) Combination of the ALCR/*alcA* ethanol switch and GAL4/VP16-UAS enhancer trap system enables spatial and temporal control of transgene expression in *Arabidopsis*. *Plant Biotechnol. J.*, **5**, 477–482.
- Kerk, N.M., Ceserani, T., Tausta, S.L., Sussex, I.M. and Nelson, T.M.** (2003) Laser capture microdissection of cells from plant tissues. *Plant Physiol.*, **132**, 27–35.
- Kiegle, E., Moore, C.A., Haseloff, J., Tester, M.A. and Knight, M.R.** (2000) Cell-type-specific calcium responses to drought, salt and cold in the *Arabidopsis* root. *Plant J.*, **23**, 267–278.
- Kim, H., Kim, Y., Yeom, M., Lim, J. and Nam, H.G.** (2016) Age-associated circadian period changes in *Arabidopsis* leaves. *J. Exp. Bot.*, **67**, 2665–2673.
- Laplaze, L., Benkova, E., Casimiro, I., et al.** (2007) Cytokinins act directly on lateral root founder cells to inhibit root initiation. *Plant Cell*, **19**, 3889–3900.
- Laplaze, L., Parizot, B., Baker, A., et al.** (2005) GAL4-GFP enhancer trap lines for genetic manipulation of lateral root development in *Arabidopsis thaliana*. *J. Exp. Bot.*, **56**, 2433–2442.
- Liu, Y.-G. and Whittier, R.F.** (1995) Thermal asymmetric interlaced PCR: automatable amplification and sequencing of insert end fragments from P1 and YAC clones for chromosome walking. *Genomics*, **25**, 674–681.
- Martí, M.C., Stancombe, M.A. and Webb, A.A.R.** (2013) Cell- and stimulus type-specific intracellular free Ca<sup>2+</sup> signals in *Arabidopsis*. *Plant Physiol.*, **163**, 625–634.
- Mockler, T., Michael, T., Priest, H., Shen, R., Sullivan, C., Givan, S., McEntee, C., Kay, S. and Chory, J.** (2007) THE DIURNAL PROJECT: Diurnal and circadian expression profiling,

model-based pattern matching and promoter analysis. *Cold Spring Harb Symp Quant Biol*, **72**, 353–363.

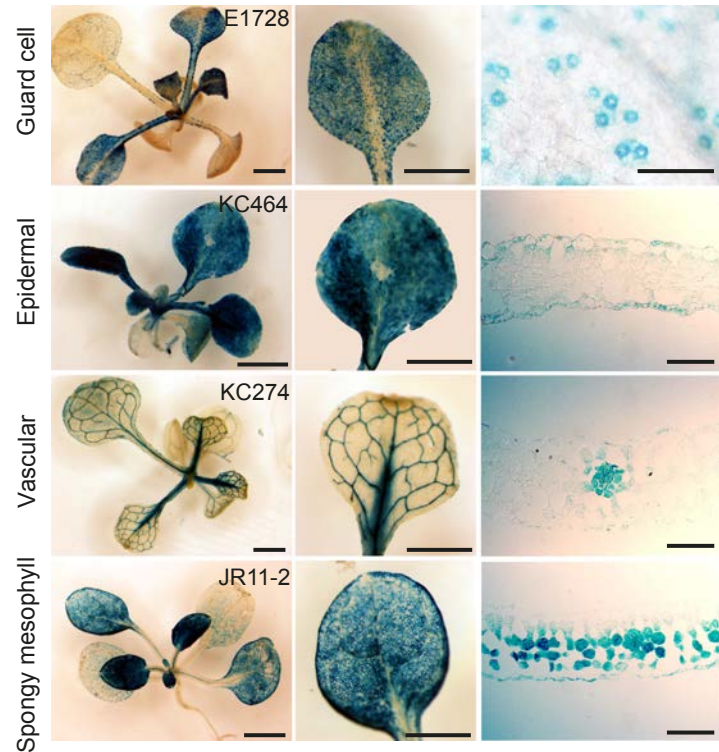
- Møller, I.S., Gilliam, M., Jha, D., Mayo, G.M., Roy, S.J., Coates, J.C., Haseloff, J. and Tester, M.** (2009) Shoot Na<sup>+</sup> exclusion and increased salinity tolerance engineered by cell type-specific alteration of Na<sup>+</sup> transport in Arabidopsis. *Plant Cell*, **21**, 2163–2178.
- Moreno-Romero, J., Santos-Gonzalez, J., Hennig, L. and Kohler, C.** (2017) Applying the INTACT method to purify endosperm nuclei and to generate parental-specific epigenome profiles. *Nat. Protoc.*, **12**, 238–254.
- Nakazono, M., Qiu, F., Borsuk, L.A. and Schnable, P.S.** (2003) Laser-capture microdissection, a tool for the global analysis of gene expression in specific plant cell types: identification of genes expressed differentially in epidermal cells or vascular tissues of maize. *Plant Cell*, **15**, 583–96.
- Para, A., Farre, E.M., Imaizumi, T., Pruneda-Paz, J.L., Harmon, F.G. and Kay, S.A.** (2007) PRR3 is a vascular regulator of TOC1 stability in the Arabidopsis circadian clock. *Plant Cell*, **19**, 3462–3473.
- Radoeva, T., Hove, C.A. Ten, Saiga, S. and Weijers, D.** (2016) Molecular Characterization of Arabidopsis GAL4/UAS Enhancer Trap Lines Identifies Novel Cell-Type-Specific Promoters. *Plant Physiol.*, **171**, 1169–1181.
- Reynoso, M.A., Pauluzzi, G.C., Kajala, K., et al.** (2018) Nuclear Transcriptomes at High Resolution Using Retooled INTACT. *Plant Physiol.*, **176**, 270–281.
- Rodrigues, A., Adamo, M., Crozet, P., et al.** (2013) ABI1 and PP2CA phosphatases are negative regulators of Snf1-related protein kinase1 signaling in Arabidopsis. *Plant Cell*, **25**, 3871–3884.
- Ron, M., Kajala, K., Pauluzzi, G., et al.** (2014) Hairy root transformation using *Agrobacterium rhizogenes* as a tool for exploring cell type-specific gene expression and function using tomato as a model. *Plant Physiol.*, **166**, 455–469.
- Ruijter, J.M., Ramakers, C., Hoogaars, W.M.H., Karlen, Y., Bakker, O., Hoff, M.J.B. van den and Moorman, A.F.M.** (2009) Amplification efficiency: linking baseline and bias in the analysis of quantitative PCR data. *Nucleic Acids Res.*, **37**, 1–12.
- Ryu, K.H., Huang, L., Kang, H.M. and Schiefelbein, J.** (2019) Single-cell RNA sequencing resolves molecular relationships among individual plant cells. *Plant Physiol.*, **179**, 1444–1456.
- Schulze, W.X., Reinders, A., Ward, J., Lalonde, S. and Frommer, W.B.** (2003) Interactions between co-expressed Arabidopsis sucrose transporters in the split-ubiquitin system. *BMC Biochem.*, **4**, 1–10.
- Shimizu, H., Katayama, K., Koto, T., Torii, K., Araki, T. and Endo, M.** (2015) Decentralized circadian clocks process thermal and photoperiodic cues in specific tissues. *Nat. plants*, **1**, 1–7.
- Takahashi, N., Hirata, Y., Aihara, K. and Mas, P.** (2015) A hierarchical multi-oscillator network orchestrates the Arabidopsis circadian system. *Cell*, **163**, 148–159.

- Toro-De Leon, G. Del and Kohler, C.** (2018) Endosperm-specific transcriptome analysis by applying the INTACT system. *Plant Reprod.*, **32**, 55–61.
- Truernit, E. and Sauer, N.** (1995) The promoter of the Arabidopsis thaliana SUC2 sucrose-H<sup>+</sup> symporter gene directs expression of beta-glucuronidase to the phloem: evidence for phloem loading and unloading by SUC2. *Planta*, **196**, 564–570.
- Vandesompele, J., Preter, K. De, Pattyn, F., Poppe, B., Roy, N. Van, Paepe, A. De and Speleman, F.** (2002) Accurate normalization of real-time quantitative RT-PCR data by geometric averaging of multiple internal control genes. *Genome Biol.*, **3**, 1–12.
- Wenden, B., Toner, D.L.K., Hodge, S.K., Grima, R. and Millar, A.J.** (2012) Spontaneous spatiotemporal waves of gene expression from biological clocks in the leaf. *Proc. Natl. Acad. Sci. U. S. A.*, **109**, 6757–62.
- Xu, X., Hotta, C.T., Dodd, A.N., Love, J., Sharrock, R., Lee, Y.W., Xie, Q., Johnson, C.H. and Webb, A.A.R.R.** (2007) Distinct light and clock modulation of cytosolic free Ca<sup>2+</sup> oscillations and rhythmic CHLOROPHYLL A/B BINDING PROTEIN2 promoter activity in Arabidopsis. , **19**, 3474–3490.
- Zielinski, T., Moore, A.M., Troup, E., Halliday, K.J. and Millar, A.J.** (2014) Strengths and limitations of period estimation methods for circadian data. *PLoS One*, **9**, 1–26.

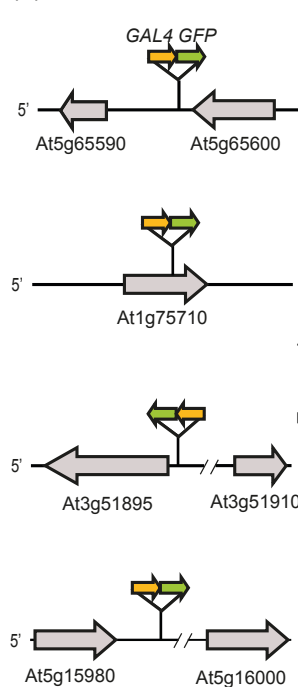




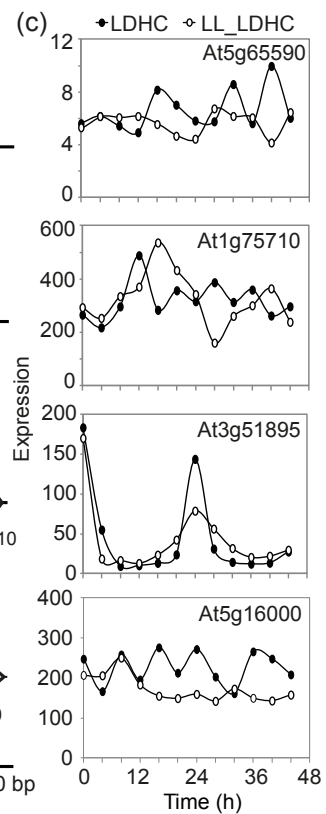
(a)



(b)



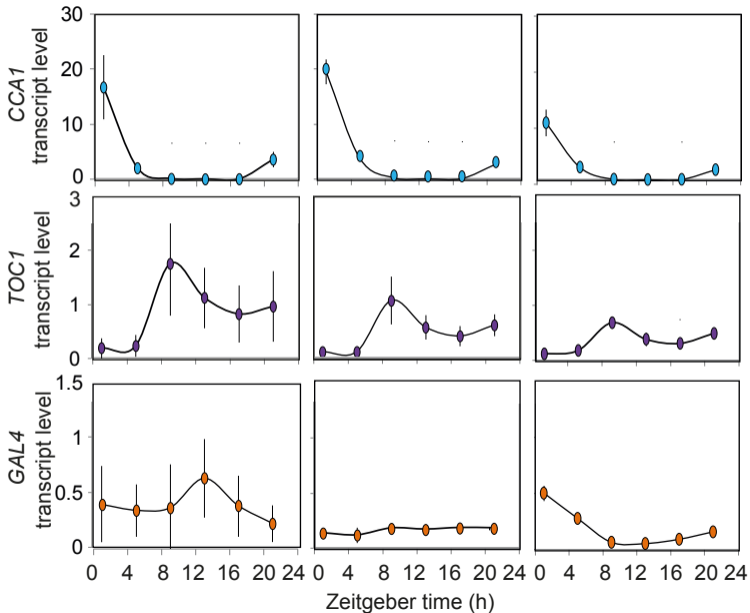
(c)



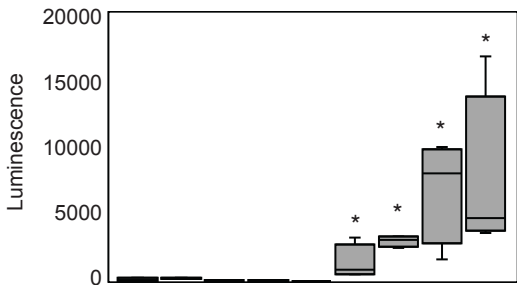
JR11-2 (mesophyll)

KC464 (epidermal)

KC274 (vascular)



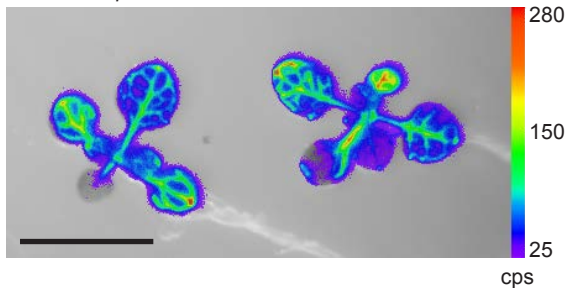
(a)

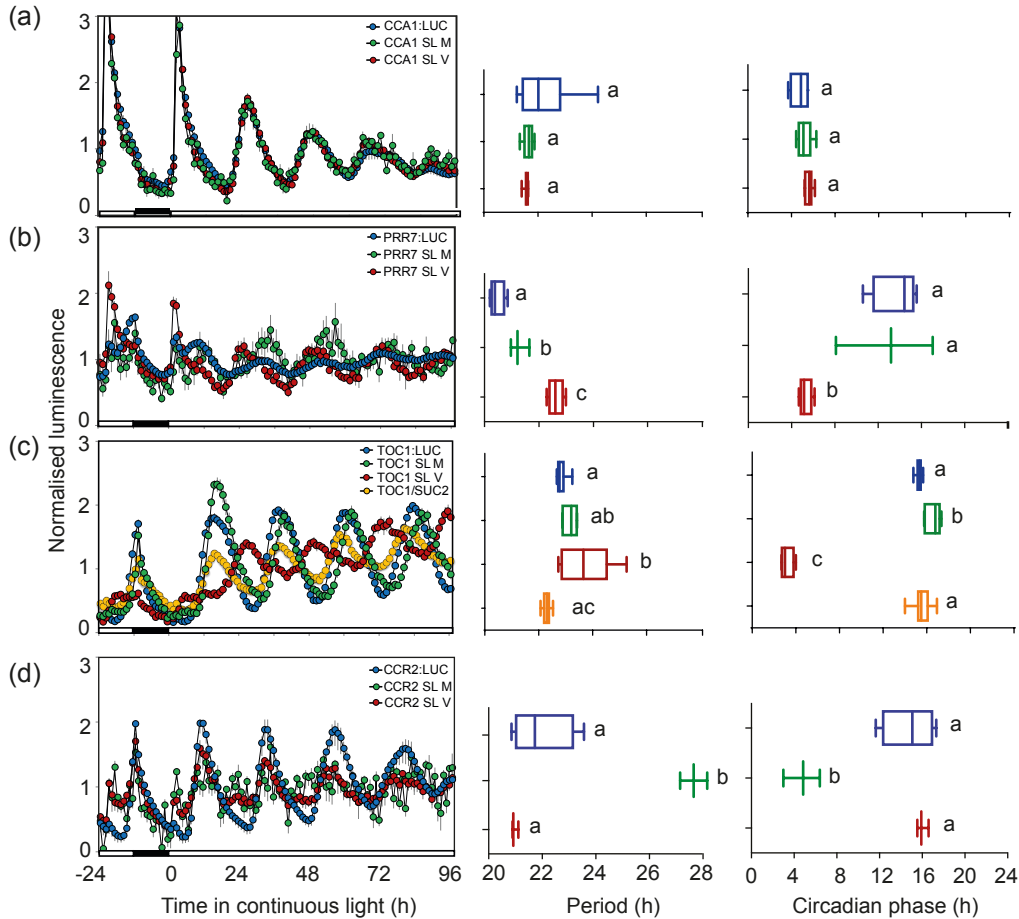


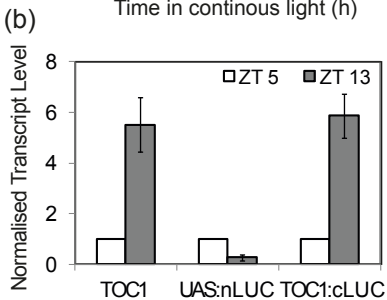
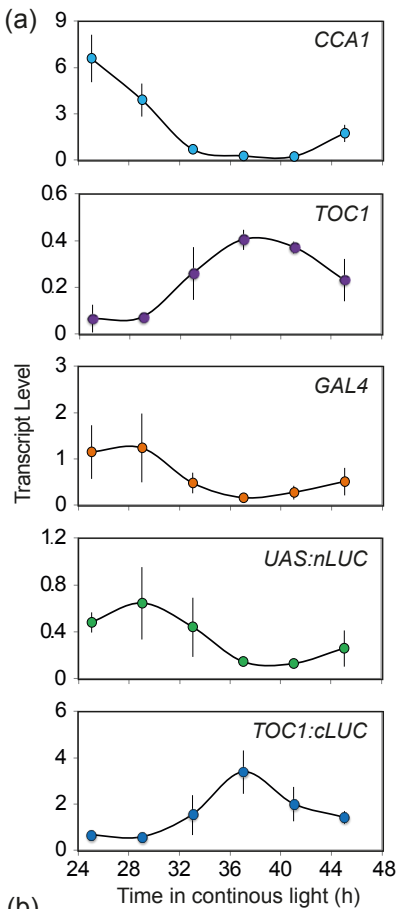
<i>CCA1p:cLUC</i>	-	+	-	-	-	+	+	-	-
<i>TOC1p:cLUC</i>	-	-	+	-	-	-	-	+	+
<i>UAS:nLUC</i>	-	+	+	+	+	+	+	+	+
mesophyll <i>GAL4</i>	-	-	-	+	-	+	-	+	-
vascular <i>GAL4</i>	-	-	-	-	+	-	+	-	+

(b)

*TOC1p:cLUC* / *UAS:nLUC* / vascular *GAL4*







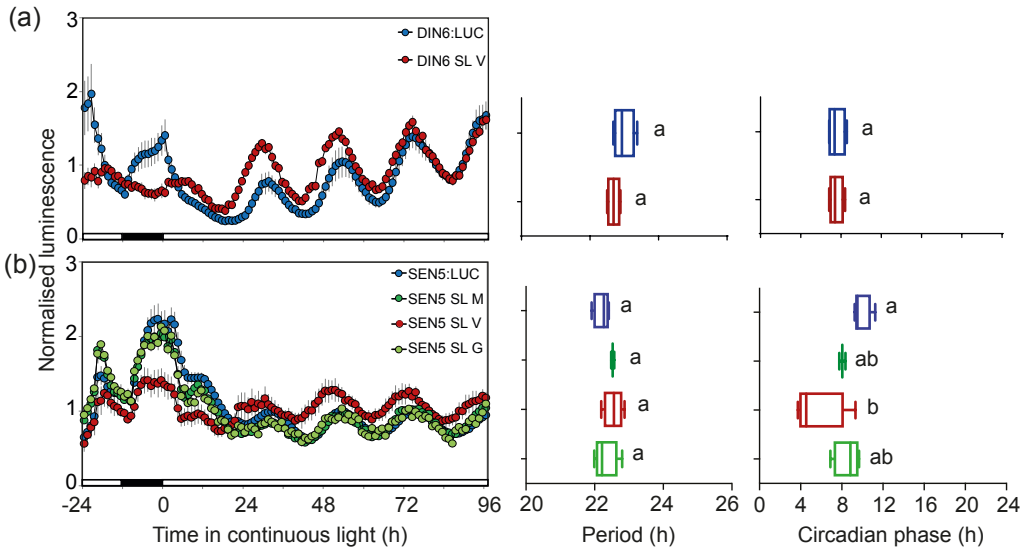


**Table S1.** List of published GAL4 enhancer trap lines compatible with the ETSLA system

Line/ABRC number	Expression Pattern		References
	Root	Shoot	
J0121/N9090	Xylem pole pericycle cells	Young leaf primordia	Laplaze <i>et al.</i> , 2005; Radoeva <i>et al.</i> , 2016
J0192	Lateral root primordia		Laplaze <i>et al.</i> , 2005
J2772	Root cap, lateral root primordia, base of lateral roots		Laplaze <i>et al.</i> , 2005
Q850	Root cap, lateral root primordia		Laplaze <i>et al.</i> , 2005
N9113		All tissues	Jia <i>et al.</i> , 2007
N9093	Distal root and root-hypocotyl junction		Jia <i>et al.</i> , 2007
N9195	Some specific tissues of the root	Leaves	Jia <i>et al.</i> , 2007
E1728	nd	Guard cells	Dodd <i>et al.</i> , 2006; Gardner <i>et al.</i> , 2009
E2036	nd	Guard cells	Gardner <i>et al.</i> , 2009
E292	nd	Guard cells	Gardner <i>et al.</i> , 2009
E361	Epidermis, cortex	Guard cells, epidermis, mesophyll, cortex, apical meristem	Gardner <i>et al.</i> , 2009
E551	nd	Guard cells, trichomes, epidermis	Gardner <i>et al.</i> , 2009
E566	nd	Guard cells, trichomes, apical meristem	Gardner <i>et al.</i> , 2009
E910	nd	Guard cells, trichomes, epidermis	Gardner <i>et al.</i> , 2009
E994	Epidermis, vasculature, root tip	Guard cells, apical meristem	Gardner <i>et al.</i> , 2009



J1512	Cortex	Guard cells	Gardner <i>et al.</i> , 2009
KS019	Epidermis	Guard cells, apical meristem	Gardner <i>et al.</i> , 2009
Q1621	Epidermis, vasculature	Guard cells, apical meristem	Gardner <i>et al.</i> , 2009
Q1622	Vasculature	Guard cells	Gardner <i>et al.</i> , 2009
Q2480	Epidermis, cortex, root tip	Guard cells	Gardner <i>et al.</i> , 2009
Q2481	Epidermis, cortex, root tip	Guard cells	Gardner <i>et al.</i> , 2009
J2103	Epidermis, vasculature, root tip	Guard cells, epidermis	Gardner <i>et al.</i> , 2009
R010/11	Epidermis	Epidermis	Gardner <i>et al.</i> , 2009
Q2610	All root tissues		Waki <i>et al.</i> , 2013
Q0990/N9217	Vasculature	nd	Radoeva <i>et al.</i> , 2016
Q2500/N9135	Ground tissue, pericycle and QC	Cotyledon junction and guard mother cell	Radoeva <i>et al.</i> , 2016
J0571/N9094	Ground tissue, some QC cells	Guard and pavement cells	Radoeva <i>et al.</i> , 2016
J2731	Cells above QC	Guard and pavement cells	Radoeva <i>et al.</i> , 2016
M0148/N9303	Pericycle cells	Cells surrounding SAM	Radoeva <i>et al.</i> , 2016
M0164/N9307	Pericycle	Shoot vasculature	Radoeva <i>et al.</i> , 2016
M0167/N9308	nd	Cotyledon junction	Cary <i>et al.</i> , 2002; Radoeva <i>et al.</i> , 2016
M0223/N9336	nd	Cotyledon junction	Cary <i>et al.</i> , 2002; Radoeva <i>et al.</i> , 2016
J1092/N9147	Root apical meristem, LRC	nd	Radoeva <i>et al.</i> , 2016

J3281/N9128	Young Vasculature tissue, columella cells	nd	Radoeva <i>et al.</i> , 2016
J3411/N9131	Root apical meristem, LRC	nd	Radoeva <i>et al.</i> , 2016
M0028/N9274	Columella cells	nd	Radoeva <i>et al.</i> , 2016
Q0680/N9209	Columella cells	nd	Radoeva <i>et al.</i> , 2016
Q1630/N9227	Columella cells	nd	Radoeva <i>et al.</i> , 2016
Q0171/N9207	Root cap	nd	Radoeva <i>et al.</i> , 2016
RM1000	Leaf margins	nd	Radoeva <i>et al.</i> , 2016
J2501/N9121	nd	nd	Radoeva <i>et al.</i> , 2016
J2661/N9187	nd	nd	Radoeva <i>et al.</i> , 2016
M0136/N9302	nd	nd	Radoeva <i>et al.</i> , 2016
M0171		Suspensor cells	Radoeva <i>et al.</i> , 2019

nd: not detected

**Table S2.** Summary of transgenic lines used in this study.

ETSLA line	Parent 1	Parent 2	Period (mean $\pm$ SD)	Phase (mean $\pm$ SD)	RAE (mean $\pm$ SD)	Experiment
CCA1p:LUC	n/a	n/a	22.2 $\pm$ 1.1	4.8 $\pm$ 0.79	0.31 $\pm$ 0.07	Fig 4a
CCA1p:LUC	n/a	n/a	22.3 $\pm$ 0.77	3.7 $\pm$ 1.0	0.25 $\pm$ 0.16	-
CCA1p-V-LUC F1	CCA1p:AC/UAS:JN T3 (A3850/52)	KC274	21.6 $\pm$ 0.08	5.6 $\pm$ 0.33	0.29 $\pm$ 0.02	Fig 4a
CCA1p-V-LUC F1	CCA1p:AC T1 (A3420)	UAS:JN/KC274 T1 (A3727)	22.2 $\pm$ 0.19	5.0 $\pm$ 0.92	0.33 $\pm$ 0.13	-
CCA1p-M-LUC F1	CCA1p:AC/UAS:JN T3 (A3850/52)	JR11-2	21.6 $\pm$ 0.18	5.2 $\pm$ 0.63	0.41 $\pm$ 0.07	Fig 4a
CCA1p-M-LUC F1	CCA1p:AC T1 (A3420)	UAS:JN/JR11-2 T1 (A3740)	22.0 $\pm$ 0.17	6.7 $\pm$ 0.45*	0.70 $\pm$ 0.15	-
PRR7p:LUC	n/a	n/a	20.5 $\pm$ 0.28	13.8 $\pm$ 2.2	0.27 $\pm$ 0.05	Fig 4b
PRR7p:LUC	n/a	n/a	21.5 $\pm$ 1.0	14.2 $\pm$ 2.5	0.13 $\pm$ 0.05	-
PRR7p-V-LUC F1	PRR7p:AC T1 (A3922)	UAS:JN/KC274 T1 (A3727)	22.6 $\pm$ 0.29	5.3 $\pm$ 0.63*	0.24 $\pm$ 0.04	Fig 4b
PRR7p-V-LUC F1	PRR7p:AC T2 (A3922)	UAS:JN/KC274 T1 (A3738)	22.4 $\pm$ 0.29*	8.5 $\pm$ 1.1*	0.28 $\pm$ 0.12	-
PRR7p-M-LUC F1	PRR7p:AC T1 (A3922)	UAS:JN/JR11-2 T1 (A3743)	21.3 $\pm$ 0.34*	12.8 $\pm$ 4.5	0.42 $\pm$ 0.10	Fig 4b
PRR7p-M-LUC F1	PRR7p:AC T2 (A3922/4112)	UAS:JN/JR11-2 T1 (A3740)	23.4 $\pm$ 1.1	12.9 $\pm$ 0.21	0.37 $\pm$ 0.17	-
TOC1p:LUC	n/a	n/a	22.8 $\pm$ 0.19	15.3 $\pm$ 0.26	0.08 $\pm$ 0.01	Fig 4c
TOC1p:LUC	n/a	n/a	22.6 $\pm$ 0.38	17.3 $\pm$ 0.85	0.18 $\pm$ 0.06	-
TOC1/SUC2 TSLA	n/a	n/a	22.0 $\pm$ 0.14	15.6 $\pm$ 0.86	0.17 $\pm$ 0.02	Fig 4c
TOC1p-V-LUC F2 (A5073)	TOC1p:AC/UAS:JN T3 (A3452)	KC274	23.7 $\pm$ 0.99*	3.2 $\pm$ 0.58*	0.28 $\pm$ 0.11	Fig 4c

TOC1p-V-LUC F1	TOC1p:AC/UAS:JN T3 (A3942/49)	KC274	22.2 ± 0.73	7.8 ± 3.2*	0.36 ± 0.10	-
TOC1p-M-LUC F2 (A5078)	TOC1p:AC/UAS:JN T3 (A3452)	JR11-2	23.2 ± 0.26	16.6 ± 0.66*	0.15 ± 0.03	Fig 4c
TOC1p-M-LUC F1	TOC1p:AC/UAS:JN T3 (A3942/49)	JR11-2	23.4 ± 1.2	14.1 ± 3.8	0.52 ± 0.24	-
CCR2p:LUC	n/a	n/a	22.0 ± 1.2	14.8 ± 2.5	0.28 ± 0.04	Fig 4d
CCR2p:LUC	n/a	n/a	22.9 ± 0.77	14.5 ± 0.99	0.22 ± 0.04	-
CCR2p-V-LUC F1	CCR2p:AC T1 (A3433)	UAS:JN/KC274 T1 (A3727)	21.0 ± 0.12	16.0 ± 0.53	0.44 ± 0.04	Fig 4d
CCR2p-V-LUC F1	CCR2p:AC T1 (A3433)	UAS:JN/KC274 T1 (A3739)	22.0 ± 0.35	10.3 ± 0.51*	0.22 ± 0.01	-
CCR2p-M-LUC F1	CCR2p:AC T1 (A3433)	UAS:JN/JR11-2 T1 (A3740)	27.7 ± 0.71*	4.8 ± 1.7*	0.77 ± 0.21	Fig 4d
CCR2p-M-LUC F1	CCR2p:AC T1 (A3433)	UAS:JN/JR11-2 T1 (A3729/37/40)	20.5 ± 0.12*	20.6 ± 0.81*	0.42 ± 0.14	-
DIN6p:LUC	n/a	n/a	23.0 ± 0.29	7.5 ± 0.79	0.35 ± 0.12	Fig 7a
DIN6p:LUC	n/a	n/a	22.0 ± 0.24	11.3 ± 1.3	0.10 ± 0.04	-
DIN6p-V-LUC F1	DIN6p:AC T2 (A3972)	UAS:JN/KC274 T1 (A3738)	22.7 ± 0.16	7.5 ± 0.66	0.13 ± 0.05	Fig 7a
DIN6p-V-LUC F1	DIN6p:AC T2 (A3972)	UAS:JN/KC274 T1 (A3727/38)	22.1 ± 0.13	9.7 ± 1.0	0.20 ± 0.05	-
SEN5p:LUC	n/a	n/a	22.2 ± 0.24	9.9 ± 0.92	0.10 ± 0.02	Fig 7b
SEN5p-V-LUC F1 (A4856-9)	SEN5p:AC/UAS:JN T3 (A3505)	KC274	22.6 ± 0.28	5.5 ± 2.6*	0.21 ± 0.05	Fig 7b
SEN5-M-LUC F1 (A4860)	SEN5p:AC/UAS:JN T3 (A3505)	JR11-2	22.5 ± 0.06	8.1 ± 0.42	0.15 ± 0.02	Fig 7b
SEN5p-G-LUC F1 (A4851-55)	SEN5p:AC/UAS:JN T3 (A3505)	E1728	22.3 ± 0.35	8.6 ± 1.3	0.32 ± 0.06	Fig 7b

\* Period and phase estimates significantly different from control by one-way ANOVA with Tukey's post-hoc test (P < 0.05).

**Table S3.** Sequences of primers used in this study.

Primer Name	Primer Sequence (5'-3')	Purpose
AC-XbaI_F	<u>AAATCTAGAGGATCCCCGGTACCATG</u>	GWp:AC construct
AC-SpeI_R	<u>AAACTAGTTTACACGGCGATCTTTCCG</u>	GWp:AC construct
PRR7p_F	CACCTGTCGATATGTCCGAGTGGT	PRR7:AC construct
PRR7p_R	CACACCAACTCTGCTTCGCTGAA	PRR7:AC construct
CCR2p-HindIII_F	<u>AAAAAAGCTTAGCGAGCCATCTTCATAC</u>	CCR2:AC construct
CCR2p-HindIII_R	<u>AAAAAAGCTTTGAAATTTGAAAAGAAGATCTA</u>	CCR2:AC construct
DIN6p_F	CACCCTTAACTATAACACAAAGAC	DIN6:AC construct
DIN6p_R	GTTTTTTTTTTGAAGAAAGTGAA	DIN6:AC construct
SEN5p_F	CACCACCGTGTCTCTCAAGTTA	SEN5:AC construct
SEN5p_R	CGTTTTCTTTGTCTTTGATTAATCC	SEN5:AC construct
JN-BamHI_F	<u>AAAGGATCCCCAAAGGTACCATGTAC</u>	UAS:JN construct
JN-SacI_R	<u>AAAGAGCTCTTATCCATCCTTGTC AATCAA</u>	UAS:JN construct
LUC+-XbaI_F	<u>AAATCTAGAATGGAAGACGCCAAAAACAT</u>	pEarleyGate301-LUC+ construct
LUC+-XbaI_R	<u>ATATCTAGATTACACGGCGATCTTTCCG</u>	pEarleyGate301-LUC+ construct
AD1	(AGCT)GTCGA(GC)(AT)GA(AGCT)A(AT)GAA	TAIL PCR
GAL4131REV	GACACTTGCGC GACTTCGGCTTCTTC	TAIL PCR
GAL499REV	CACTTGAGTTCTTGAGGCGGGCAGAT	TAIL PCR
GAL445REV	AGCTTCATTGTTGGATCCGTTCTCT	TAIL PCR
LB5102FWD	GGAACAACACTCAACCCTATCTCGGG	TAIL PCR
LB5147FWD	GGGATTTTGCCGATTTTCGGAACCACC	TAIL PCR
LB5199FWD	GCAAACCAGCGTGGACCGCTTGCTGC	TAIL PCR
At5g65590_F	TCACCGTTGTC ACTCTCGAA	sequence T-DNA flanking region

At1g75710_F	GTCACATGATCGTTGACCCG	sequence T-DNA flanking region
At3g51910_R	TGCAACCGTTACCAAAACCC	sequence T-DNA flanking region
At5g15980_F	GGAAGTGAACGAGGAGGAACA	sequence T-DNA flanking region
CCA1_F	GATGATGTTGAGGCGGATG	qRT-PCR
CCA1_R	TGGTGTAACTGAGCTGTGAAG	qRT-PCR
TOC1_F	TCTTCGCAGAATCCCTGTGAT	qRT-PCR
TOC1_R	GCTGCACCTAGCTTCAAGCA	qRT-PCR
GAL4_F	GACATCTGCCGCCTCAAG	qRT-PCR
GAL4_R	GCGACACTCCAGTTGTTCT	qRT-PCR
IPP2_F	GTATGAGTTGCTTCTCCAGCAAAG	qRT-PCR
IPP2_R	GAGGATGGCTGCAACAAGTGT	qRT-PCR
PP2AA3_F	TAACGTGGCCAAAATGATGC	qRT-PCR
PP2AA3_R	GTTCTCCACAACCGCTTGGT	qRT-PCR
UAS:nLUC_F	GAAGAGATACGCCCTGGTTCCT	qRT-PCR
UAS:nLUC_R	CCGATAAATAACGCGCCCAA	qRT-PCR
TOC1p:cLUC_F	TTGCTCCAACACCCCAACAT	qRT-PCR
TOC1p:cLUC_R	TCATCGTCTTTCCGTGCTCC	qRT-PCR
GAL4FP	GACATCTGCCGCCTCAAG	<i>in situ</i> probe synthesis
GAL4RP	GCTCGAGACGGTCAACTG	<i>in situ</i> probe synthesis
M13 (-40)	GTTTTCCAGTCACGAC	<i>in situ</i> probe synthesis